

Lawrence Berkeley National Laboratory

LBL Publications

Title

THE SURFACE CHEMICAL BOND

Permalink

<https://escholarship.org/uc/item/8gq9r7xw>

Author

Somorjai, G.A.

Publication Date

1976-08-01

0 0 4 6 0 3 4 0 7

Presented at the Amsterdam Congress
Aug. -76: 'Exploring the Chemical Bond',
Amsterdam, Holland, August 30 -
September 1, 1976; also Submitted to
Angewandte Chemie

LBL-5451

c. 1

THE SURFACE CHEMICAL BOND

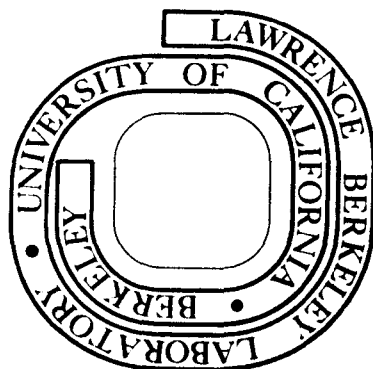
G. A. Somorjai

August 26, 1976

Prepared for the U. S. Energy Research and
Development Administration under Contract W-7405-ENG-48

For Reference

Not to be taken from this room



LBL-5451

c. 1

DISCLAIMER

This document was prepared as an account of work sponsored by the United States Government. While this document is believed to contain correct information, neither the United States Government nor any agency thereof, nor the Regents of the University of California, nor any of their employees, makes any warranty, express or implied, or assumes any legal responsibility for the accuracy, completeness, or usefulness of any information, apparatus, product, or process disclosed, or represents that its use would not infringe privately owned rights. Reference herein to any specific commercial product, process, or service by its trade name, trademark, manufacturer, or otherwise, does not necessarily constitute or imply its endorsement, recommendation, or favoring by the United States Government or any agency thereof, or the Regents of the University of California. The views and opinions of authors expressed herein do not necessarily state or reflect those of the United States Government or any agency thereof or the Regents of the University of California.

0 0 0 0 4 6 0 3 4 0 8

LBL 5451

THE SURFACE CHEMICAL BOND

G. A. Somorjai

Materials and Molecular Research Division, Lawrence Berkeley Laboratory
and Department of Chemistry, University of California
Berkeley, California 94720

Introduction

The nature of the surface chemical bond that forms between adsorbed atoms and/or molecules on the surface of a solid has been the subject of extensive speculation over the past several decades. The formation and breaking of these bonds are controlling processes in heterogenous catalysis in adhesion and lubrication to name a few of many important phenomena that take place at surfaces. Only over the past decade have techniques become available that permit investigation of the surface bond on the molecular level. These techniques are surface crystallography by low-energy electron diffraction (LEED) that determine the location, bond distance and bond angles of the adsorbates and electron spectroscopies (Ultraviolet photoelectron spectroscopy (UPS), x-ray photoelectron spectroscopy (XPS), and electron absorption spectroscopy) that permit studies of the electronic structure of the substrate and adsorbate and the vibrational frequencies associated with the various surface bonds. These techniques are still under development and have been applied to only a few adsorbate systems. Yet, as a result, a model of the surface chemical bond emerges. It appears that the bonding in the solid surface-adsorbed molecule (atom) system is localized among a few neighboring atoms that can be viewed as a cluster. The adsorbed species are bound to one or several of the nearest surface atoms in well-defined configurations corresponding to maximized bond energy. Correlations between chemical bonding at the surface and bonding in multinuclear clusters of atoms have been found and will be discussed later.

In this paper we shall first discuss the structure and charge density

of solid surfaces as it is revealed by low-energy electron diffraction and electron spectroscopy studies. These surface properties determine primarily the nature of the surface bond. Then we shall review the adsorbate systems where bonding information has become available.

Atomic Structure of Clean Solid Surfaces

The atoms at the surface are in an asymmetric environment. They are surrounded by atoms in the surface layer and from beneath but there are no atoms above them. This surface environment has also lower symmetry than that provided for atoms in the bulk. The structural asymmetry experienced by atoms at the surface have a major effect that leads to surface reconstruction: atoms in the surface may move into new equilibrium positions that provide higher symmetry or greater overlap of available bonding orbitals.

a) Surface reconstruction. There are several types of surface reconstruction observed for clean solid surfaces. Many surfaces have atomic structures that are different from that expected from the projection of the x-ray bulk unit cell. The surface atoms assume new equilibrium positions by out-of-plane buckling or by relaxing inward (contraction) that often results in entirely different ordered surface structures. An example of this is shown in Fig. 1. The diffraction pattern and schematic representation shown here are characteristic of the surface structure of the (100) crystal face of platinum. This surface exhibits the so-called (5x1) surface structure. (1,2) There are two perpendicular domains of this structure and there are $1/5$, $2/5$, $3/5$ and $4/5$ order spots between the (00) and (10) diffraction beams. The surface structure appears to be stable at all temperatures from 25°C to the melting point although at elevated temperatures impurities from the bulk can come to the surface and cause a transformation

-3-

of the structure to the impurity stabilized (1x1) surface structure. Preliminary calculations by Clark, et al⁽³⁾ and in this laboratory indicate that a model for Pt (100) in which the surface atoms assume a distorted hexagonal configuration by out-of-plane buckling is favored. The apparent (5x1) unit cell is then the result of the coincidence of the atomic positions of atoms in the surface, i.e., in the distorted hexagonal layer, with atoms of the undistorted second layer below. The (100) crystal faces of gold⁽⁴⁾ and iridium⁽⁵⁾ that are neighbors of platinum in the periodic table exhibit the same surface reconstruction and the same surface structure as that of platinum that is shown in Fig. 1. The (110) crystal faces of these three elements are also restructured⁽⁶⁾ and exhibit different unit cells than that expected from the bulk x-ray structure. On the other hand, the (111) crystal face of these three metals appears to have the same surface structure as that indicated by the bulk unit cell.

For semi-conductors, most crystal planes that have been studied show reconstruction.⁽⁷⁾ Monatomic and diatomic semi-conductor surfaces have been investigated in large numbers and surface reordering has been observed for most of them. Frequently there are changes of surface structure with temperature that are often irreversible.

For many metal surfaces, the distance between the uppermost two layers, i.e., the z-spacing, is equal to that of the bulk value to within the estimated accuracy of about five percent. However, the Al (110),⁽⁸⁾ Mo (100)⁽⁹⁾ and W (100)⁽¹⁰⁾ surfaces seem to show substantial contraction in the upper layer z-spacing with respect to the bulk while retaining the (1x1) surface unit cell. A simple contraction or expansion of the interplanar z-spacing of this kind is usually termed a "relaxation."

For many diatomic solids there is non-stoichiometry in the surface layer, that is the surface composition may be different from that in the bulk.⁽⁷⁾ Non-stoichiometry is apparently a major factor in the observed reconstruction of the polar faces of the III-V semi-conductors such as gallium arsenide, GaAs. The (111) face, for example, would ideally have all gallium atoms at the surface bonded to arsenic atoms immediately beneath the surface while the reverse would be true of the ($\bar{1}\bar{1}\bar{1}$) face. However, the ($\bar{1}\bar{1}\bar{1}$) surface has been found to lose arsenic at elevated temperatures and this is associated with the appearance of a new surface structure, while at low temperature another surface structure is arsenic stabilized.⁽¹¹⁾ Similarly, phosphorus is found to preferentially desorb at high temperatures from the gallium phosphide's ($\bar{1}\bar{1}\bar{1}$) surface.⁽¹²⁾ On the other hand, the gallium arsenide (110) surface, which has an equal number of gallium and arsenic surface atoms, does not exhibit reconstruction. A number of studies have pointed to possible non-stoichiometry in alkali-halide crystal surfaces also upon cleavage.⁽¹³⁾ On oxide surfaces, such as aluminum oxide⁽¹⁴⁾ and vanadium pentoxide,⁽¹⁵⁾ changes in chemical composition and valency of surface atoms have been related to the formation of new surface unit cells.

Molecular crystals constitute a large and important group of materials that include most organic solids, but only very recently have the surface structures of some of these materials been investigated on an atomic scale by low-energy electron diffraction. Ice and naphthalene have been grown by vapor deposition⁽¹⁶⁾ and ordered surface structures of crystals of many other organic solids such as benzene, trioxene, n-octane, cyclohexene and methanol have been grown on metal substrates at low temperatures.⁽¹⁷⁾

Phthalocyanine crystals have been vapor-grown on ordered metal surfaces.⁽¹⁸⁾ These large molecular weight, large size organic crystals exhibit a different kind of surface reconstruction. When copper phthalocyanine was grown on the copper (111) surface, the surface structure of the growing organic crystal layer did not resemble the structure of any of the simpler crystal planes in the bulk structure of the organic crystal. It appears that the ordered metal substrate predetermined the orientation and packing of the phthalocyanine monolayer, which in turn controlled the orientation and packing of the organic layer deposited on top of it. For large molecules, such as phthalocyanine, restructuring into a more stable crystallographic arrangement requires molecular rotation and diffusion processes that are too slow under conditions of crystal growth. Thus the molecules are frozen into a surface structure that is predetermined by the structure of the substrate and the first adsorbed organic monolayer.

b) Surface irregularities. The surfaces of real solids are atomically heterogeneous and not smooth as shown schematically in Fig. 2. There are several atomic sites present simultaneously that are distinguishable by their number of nearest neighbors. The symmetry of these low coordination number sites and their charge density are different from that of the sites on the smooth surface and are different from each other. As a result, large variation in chemical bonding of adsorbates at these different sites could occur. Indeed, there is an increasing body of experimental evidence that indicate that atomic steps and kinks behave as different chemical entities at transition metal^(19,20) and semi-conductor surfaces,⁽²¹⁾ forming chemical bonds of different strengths as compared to that of the atoms on the terraces.

Preparation of surfaces with a large concentration of stable and ordered irregularities (steps and kinks) can be carried out by cutting crystal faces along high Miller index directions. ⁽²²⁾ Stepped surfaces of several metals, ⁽²³⁾ semi-conductors ⁽²⁴⁾ and oxide surfaces ⁽²⁵⁾ were prepared this way.

In order to study the surface chemical bond it is essential to carry out the investigation of structurally well-characterized solid surfaces. For this purpose single crystals of various orientations are used. Low Miller index crystal faces (111), (100) and (110) orientations of face-centered cubic metals certainly have a high density of surface atoms and the surfaces have the lowest surface free energy. Under proper conditions, these surfaces can be prepared in such a way that most of their atoms are terrace atoms. The density of steps or other irregularities are orders of magnitude lower than the total surface concentration (approximately 10^{15} atoms/cm²). At this stage of development, studies of adsorbate structure and bonding are concentrated on using atomically smooth and homogeneous surfaces such as provided by these low Miller index surfaces of cubic solids. One face of a single crystal of a clean solid provides the best surface to carry out these experiments. Thus, we shall not discuss the structural properties and adsorption characteristics of high Miller index surfaces that exhibit a large concentration of surface irregularities in this paper.

Charge Density at Clean Solid Surfaces

Let us consider an atomically smooth surface where each atom is in the same structural environment. The surface atoms have less nearest neighbors as compared to atoms in the bulk. As a result, electronic orbitals that are used for bonding of bulk atoms are available at the surface, giving rise to increased charge density. These localized unsaturated bonding orbitals are frequently called dangling bonds and the angular distribution of their charge density largely depends on the structural arrangement (packing of atoms, orientation) at the surface. There is excess free electron density at metal surfaces that is not localized at a given atom that gives rise to an induced surface dipole. The presence of this dipole is responsible for changes of the work function of metals from crystal face to crystal face. The formation of the surface dipole can be rationalized and demonstrated using the so-called jellium model. There are strong exchange correlation forces which act on the electrons in the solid due to their many-body coulomb interactions. In the metal interior each electron lowers its energy by pushing others away to form the exchange-correlation "hole". This attractive interaction is lost when the electron leaves the solid so there is a sharp potential barrier at the surface. In the jellium model the positive charge density from the ion cores is smeared out over the atomic volume and the conduction electrons are free to respond to ^{the} surface barrier potential. At the surface, however, the electrons are not totally trapped and there is a small probability to leak out in the vacuum. This charge leakage creates a dipole effect which modifies the self-consistent surface barrier potential. This dipole creates an additional electrostatic barrier for the electrons in the solid,

V_{dipole} , so that the total barrier, $V_{\text{total}} = V_{\text{exchange}} + V_{\text{dipole}}$. This gives the work function, $\phi = V_{\text{exchange}} + V_{\text{dipole}} - E_F$, where E_F is the energy at the Fermi level. Variations of the work function from crystal face to crystal face are well documented.

Surface irregularities, like atomic height steps at the surface exhibit different work functions as determined by Wagner and Besocke recently.⁽²⁶⁾ Recent theoretical studies provide firm foundation of the effect of surface heterogeneity and irregularities on the density of states at the Fermi level⁽²⁷⁾ and on the angular distribution of charge densities⁽²⁸⁾ at these low coordination number surface sites. The structural heterogeneity at the surface leads to the chemical heterogeneity, i.e., the ability of the surface to carry out complex chemical rearrangements involving the simultaneous forming and breaking of surface bonds of varied strength at the various atomic surface sites.

Techniques to Study the Surface Chemical Bond

A. Surface Crystallography by LEED^(29, 30)

A typical apparatus used for low-energy electron diffraction experiments is illustrated in Fig. 3. Ultra-high vacuum conditions (base pressure approximately 10^{-9} torr) are maintained to ensure surface cleanliness. The backscattered electrons are post-accelerated to a fluorescent screen and the diffraction pattern so produced is observed through a glass viewport. The condition of the surface under study is quite apparent from the diffraction pattern. Sharp spots are indicative of long-range order (200 \AA) on the surface. Diffuse and large spots probably signal poor ordering or the presence of adsorbed impurities. Extra diffraction spots, meaning those not expected on the basis of simple termination of the bulk lattice structure along the surface plane, indicate either a reordering,

reconstruction of the lattice in the surface region, or the presence of ordered impurity structures. Electron spectroscopy, mostly Auger electron spectroscopy that is to be described below, is routinely used to identify impurities that may be present with about one percent of a monolayer sensitivity before, during and after low-energy electron diffraction studies.

The electron energy range of 15 to 200 eV provides optimal surface sensitivity. The electrons in this range do not penetrate more than a few atomic layers before they undergo inelastic scattering events (absorption) and are lost from the diffracted (elastic) portion of the beam. Furthermore, they are rather strongly scattered in an elastic fashion by the attractive coulomb forces of the atomic nuclei and may traverse very complex trajectories (multiple or dynamical scattering) before exiting from the crystal. These considerations are, of course, quite general and also have some bearing on quantitative interpretation of various electron spectroscopies.

As outlined above, the dimensions of the surface unit cell are readily found from observations of the diffraction pattern geometry. We cannot in this manner, however, discover the arrangement of atoms or molecules in the basis of the unit cell nor ^{obtain} information concerning spacings of the atoms in the direction perpendicular to the surface plane. This essential information can be extracted from analysis of the dependence of the intensity, I , of the diffraction spots on the incident beam energy, V , so-called I - V profiles. These profiles exhibit pronounced peaks and valleys which are indicative of constructive and destructive interference of the electron waves scattered from planes parallel to the surface as the electron wavelength is varied. A rather complete quantum-mechanical description of this scattering has been achieved through the efforts of a number of theorists

in recent years, but the details are outside the scope of this discussion. It suffices here to state that an accurate description of the I-V profiles requires, in general, consideration of several orders of multiple scattering and absorption due to inelastic events and vibrational effects. The diffraction beam intensities are measured by photographing the fluorescent screen or by using other means of detection of the elastically scattered electron flux.⁽³¹⁾ The intensities are then calculated based on a scattering model in which the essential parameter to be adjusted is the atomic geometry. The assumed geometry is varied until the best fit between theory and experiment is reached. Fortunately, the calculated I-V profiles are very sensitive to geometrical spacings so that accuracy of 0.1 \AA in atomic positions have been obtained in the better calculations. This procedure has been applied to quite a number of clean surfaces and has also provided quantitative bonding information for atomic and molecular adsorbates. Alternates of this rather indirect method of analysis have not as yet proven viable.

B. Electron Spectroscopy Techniques

Techniques of electron spectroscopy that are used to determine the surface composition and bonding may be divided into two parts. a) Core-level electron spectroscopies that achieve chemical identification on the basis of the characteristic energies of atomic core states. Variations of surface chemical bonding are observed as chemical shifts of the core levels. b) Valence-level spectroscopies that are also sensitive to chemical structure. Here an electron is excited from the valence band or the chemical bond of the surface atom or adsorbate and its energy is used to learn about chemical bonding and structure at surfaces.

A) Core-level electron spectroscopies.

There are four processes involving core levels that are of importance in surface studies. 1) The first one leads to x-ray photoelectron spectroscopy (XPS).⁽³²⁾ Incident x-rays cause electron excitation from a core level into vacuums. The energy distribution of the emitted electrons is observed.

2) Incident electrons cause electron excitation from a core level to a final level above the Fermi level and in so doing, suffer an equal energy loss that is detectable. This is called energy-loss spectroscopy (ELS).⁽³³⁾

3) After the initial excitation of the core level caused by incident x-rays, electrons, ions or other means, an Auger deexcitation process occurs. The core hole is filled by a transition from a high-lying occupied level and the transition energy is transferred to another electron (Auger electron) in the same atom or in a neighboring atom which is then emitted. In Auger electron spectroscopy, the energy distribution of emitted electrons is observed.⁽³⁴⁾

4) After an initial electron excitation from a core level caused by an incident electron, the core hole is filled by a transition from a high-lying occupied level and x-rays or Auger electrons are emitted. In appearance potential spectroscopy (APS) the derivative of the intensity of emitted x-rays or Auger electrons is measured as a function of the incident electron energy.⁽³⁵⁾ At each critical value of the incident electron energy at which the energy is just sufficient to excite a core electron to vacant levels above the Fermi level, E_F , the intensity of emission suddenly increases. This is recorded as a peak in the derivative of the emission intensity.

B) Valence electron spectroscopies.

Ultra-violet photoelectron spectroscopy (UPS).⁽³⁶⁾ Using this technique, an ultra-violet photon is absorbed by a valence electron whose energy is increased by $h\nu$, making it possible for the excited electron to leave the crystal. In UPS the final state energy of the excited electron is measured, thus determining the initial state energy. $E_{\text{final}} = E_{\text{initial}} - h\nu$. Current surface work is being done at photon energies in the range of 10 to 45 eV.

C) Electron absorption spectroscopy⁽³⁷⁾

The energy losses suffered by incident electrons of 1-10 eV energy are monitored with an energy resolution of $\pm 7-20$ meV. Monochromatized incident electron beams as well as high energy resolution electron detectors are utilized in these studies. The energy losses in this energy range are due to vibrational excitations of the surface bonds. This way, C-C, C=C, C \equiv C, C-H and H-C bonds have become distinguishable and detectable. Moreover, adsorbed hydrogen atoms whose scattering cross sections are very small compared to other atoms and therefore not readily detectable by either electron spectroscopy or by LEED techniques are detectable by electron absorption spectroscopy through their stretching and bending modes of vibration with respect to atoms in the solid surface (M-H). Recent studies by Ibach et al and by Willis et al revealed the great sensitivity of this technique to the study of the surface chemical bond.

The Surface Crystallography of Adsorbed Monolayers of Atoms

The structural asymmetry and excess charge experienced by atoms at the surface have an important effect on the structure of the adsorbate substrate system. In the presence of adsorbates, bonds are formed that make optimum use of the available bonding orbitals. For small adsorbed atoms and

molecules this often leads to the formation of a close-packed adsorbate structure in which the adsorbate occupies the high symmetry atomic sites that correspond to the continuation of the bulk structure. We shall review several examples of chemisorbed structures of these types below.

For most of the over 200 surface structures of adsorbed monolayers that have been studied so far, only the two-dimensional symmetry of the diffraction pattern has been determined.⁽²⁹⁾ Thus, only the size and shape of the two-dimensional surface unit cell is known. Determination of the actual positions of the adsorbed atoms requires analysis of the intensity of the diffraction beam and has been performed only on a small number of systems, almost all for atomic adsorption and low Miller index surfaces of face-centered cubic metals. The first of these analyses was carried out by Anderson and Pendry,⁽³⁸⁾ who examined sodium adsorption on the nickel (100) crystal face and reported that the sodium atoms occupy four-coordinated sites at a distance of 0.87 \AA above the top-most nickel layer. Demuth, et al⁽³⁹⁾ have examined the overlayer structures of oxygen, sulfur, selenium and tellurium on nickel (100). On this surface they find the adsorbed atom to occupy four-coordinated bonding sites at displacements of 0.9, 1.3, 1.45 and 1.9 \AA respectively from the center of the top nickel layer. Results are also given for nickel (111) and nickel (110). Forstmann, et al⁽⁴⁰⁾ reported iodine adsorbed on Ag (111) to occupy the three-fold sites at a distance of 2.5 \AA above the top-most layer. Oxygen adsorption on tungsten⁽⁴¹⁾ and nitrogen on tungsten⁽⁴²⁾ and other body-centered cubic metals have also been studied.

Several general observations appear to be emerging from this work. Chemisorbed atoms seek an adsorption site which allows them to maximize

their coordination. The substrate-adsorbate bond length, at least for the strongly chemisorbed systems studied thus far, can be reproduced rather well by adding the metallic radius of the substrate and the single bond covalent radius of the adsorbate. This is shown in Table 1, which lists the experimentally determined bond length and the predicted bond length obtained by summing the covalent radii. In most cases, the difference is within the 0.1 \AA accuracy claimed for the experimental determination and in no case is the discrepancy greater than ten percent. This result suggests that the chemisorption bond of the small adsorbate atoms studied so far is basically covalent in character, which means that theoretical treatment in terms of localized surface complexes and clusters should be applicable to their chemisorption.

The small adsorbate atoms that are listed in Table 1 invariably occupy sites of the highest symmetry. These sites would also be the location of the next layer of metal atoms if we were to continue building up the solid layer by layer. The adsorbate-metal atom bond distance is equal, within the experimental accuracy, to the sum of the covalent radii of the two atoms. There are other types of surface bonding however, that are neither simple nor readily rationalized using simple chemical arguments. For example, when oxygen adsorbs on nickel (110), the best agreement with experiment is obtained assuming that oxygen atoms are lying in a two-fold bridge site between 1.41 and 1.51 \AA above the nickel layer.⁽⁴³⁾ This is clearly not the highest coordination site on the surface. The fact that bridge bonding is preferred suggests that atomic oxygen bonds to two adjacent nickel atoms via the oxygen p_x and p_y atomic orbitals. The bond angles and atomic distances are very close to what one expects from X_2O compounds, where X is the metal atom.

Another example of unusual bonding is detected in studies of hydrogen adsorption to the nickel (110) surface recently. A new surface structure forms and surface crystallography studies indicated that this unit cell is a consequence of the restructuring of the nickel (110) surface as a result of hydrogen chemisorption and not due to ordering of the hydrogen adsorbate.⁽⁴³⁾ The surface structure model that gave best fit to the experimental data consists of distorting the nickel surface atoms so as to produce the new (1x2) periodicity. This is carried out by simple depression or raising of every alternate row of nickel atoms in one direction, or a pair-wise distortion of every alternate row of nickel atoms in the plane of the surface. The optimal agreement with experimental curves is obtained by a 0.1 \AA compression of the surface layer and a 0.1 \AA alternate displacement of the rows of nickel atoms in the $[\bar{1}\bar{1}0]$ direction.

Another example of unusual structure comes from studies of the titanium-oxygen system. It has been reported recently⁽⁴⁴⁾ that upon chemisorption, oxygen atoms are located below the first layer of titanium atoms in the (0001) surface. There is little doubt that future studies will reveal the richness and complexity of surface bonding and will yield many unexpected bonding configurations.

Studies of Hydrocarbon Bonding to Metal Surfaces

A. The Surface Crystallography of Acetylene on Pt (111)

Acetylene, C_2H_2 , forms a (2x2) overlayer on the platinum (111) crystal surface. In recent experimental studies, Stair and Somorjai and Kesmodel, et al have reported the LEED I-V profiles for the acetylene-platinum system.^(45,46) In particular, two different (2x2) structures of adsorbed acetylene were identified, which we refer to briefly as stable and metastable state and which have been interpreted as involving different chemical bonding. The metastable

(2x2) structure is observed to form initially at low exposure (one Langmuir = 10^{-6} torr-sec) of C_2H_2 at room temperature but transforms in one hour to the stable (2x2) structure upon gentle heating to $100^{\circ}C$. Both structures are characterized by the same (2x2) surface unit cell and involve the same carbon coverage as determined by Auger electron spectroscopic analysis. However, they are readily distinguishable by their different I-V characteristics.

Let us examine the various modes of bonding of acetylene to platinum in the context of high symmetry bonding sites available on the (111) face of an f.c.c. crystal. As illustrated in Fig. 4, we distinguish four sites designated as: a) one-coordinate π ; b) di- σ ; and c) bridging (sometimes referred to as μ -bridging) and d) triangular complexes. We have indicated for each site only those surface metal atoms expected to have significant metal-carbon interaction. It is natural to discuss these surface geometries in terms of structural analogies of organo-metallic complexes. In these terms, the one-coordinate π complex, a), involves the interaction of one or both sets of π orbitals of the acetylene molecule with a single metal surface atom. The bridging site, c), utilizes both sets of π orbitals to bond with two surface atoms; both a) and c) in principle entail little rehybridization of the molecule since essentially undistorted π orbitals would be involved. However, the di- σ bond, b), implies $sp \rightarrow sp^2$ rehybridization and the formation of two carbon metal σ bonds accompanied by large hydrogen cis bending (CCH angle = 120°). This possibility has received serious consideration in the catalysis literature. Finally, the triangular structure, d), commonly found in tri-nuclear metal alkyne complexes illustrates a mode

of bonding loosely referred to in terms of both σ and μ bonds. As discussed below, we find this triangular geometry to be the favored arrangement in the stable structure.

In Table II we cite various organo-metallic compounds demonstrating the four geometries we have considered. Let us note that we have examined only high symmetry structures having the C-C axis parallel to the platinum surface. We consider it unlikely that large distortions from planarity, e.g., end-on bonding characteristic of metal carbonyls would occur for chemisorbed acetylene as it leads to minimum overlap of bonding molecular orbitals. Furthermore, in previous work it was noted that a rather closely packed layer of planar acetylene molecules is consistent with the observed (2x2) unit cell. The possibility of dissociation of acetylene to CH fragments bound to the surface in a (2x2) configuration was ruled out based on experimental evidence to be discussed below.

In Figs. 5 and 6 we compare selected results for di- σ bridging and triangular structures. On the (111) surface of f.c.c. crystals (abc stacking) there are two inequivalent triangular sites distinguished by the presence or absence (hole site) of a second layer substrate atom located beneath the center of the triangle formed by substrate atoms in the top-most layer. The hole site corresponds to the site that would be filled in the formation of an additional substrate layer and this is also found in the calculations to be the particular triangular site giving the optimum agreement for the location of C_2H_2 molecules in the acetylene overlayer. The z-distance of 1.9 Å employed in these comparisons was optimum for all three structures and all diffraction angles to within $\pm 0.1^\circ$ Å.

Analysis of Figs. 5 and 6 shows that the triangular geometry gives

consistently better agreement than either the bridging or di- σ geometries. The one-coordinate π complex can be ruled out readily as well. We should also note the effects of scattering by the hydrogen atoms in a trial calculation for the bridging structure at normal incidence.

The intensity profiles indicate that major $sp \rightarrow sp^2$ rehybridization of acetylene does not occur. The CCH bond angle appears to be greater than 150° for acetylene in the adsorbed state. If rehybridization occurred, the CCH bond angle of 120° would be expected. For a z-distance of 1.9 \AA C-Pt distances of 2.2 \AA are found for C_2H_2 centered on the triangular site. This value is very close to the predicted covalent bond distance of 2.16 \AA .

We have been able to distinguish amongst various proposed bonding models for acetylene adsorption on the Pt (111) surface using dynamical analysis of low-energy electron diffraction intensity profiles. We have found that bonding of acetylene in a triangular site on the Pt (111) surface is the stable and preferred configuration. It is interesting to note that this same bonding geometry is exhibited in tri-nuclear metal alkyne clusters; moreover, the average C-Pt distance we find is similar to that determined for the osmium tri-nuclear cluster (Table II), the osmium covalent radius being only 0.04 \AA shorter than that of platinum. Although we cannot detect a small C-C bond length change we do anticipate a C-C bond stretch of about 0.1 \AA to occur for acetylene adsorption judging from the C-C length found in x-ray crystal structure determinations of the metal alkyne clusters.

We have also found encouraging evidence that CCH angle bending may be studied by the dynamical technique in spite of the fact that electron scattering by hydrogen is relatively weak.

B. Studies of Other Hydrocarbons by Electron Spectroscopy

The bonding and the composition of C_2H_4 was studied on the nickel (111) crystal face by (UPS).⁽⁴⁷⁾ At $100^\circ K$, the organic molecule adsorbs by bonding via its π orbitals to the metal surface. On heating to $230^\circ K$, C_2H_4 dehydrogenates to form C_2H_2 that is bound with even stronger π bonds to the nickel surface. (UPS) could monitor changes in bonding caused by the activated dehydrogenation that occurs as a function of temperature. Chemisorption involved predominantly π -d bonding, thus rehybridization of the adsorbed molecule does not seem to occur.

Similar studies were carried out with C_2H_4 adsorbed on the W (110) crystal face.⁽⁴⁸⁾ At $300^\circ K$, the molecule dehydrogenates upon adsorption to form C_2H_2 that π bonds to the metal. As the surface temperature is increased to $500^\circ K$, breaking of the carbon-hydrogen bond occurs and the C_2 fragments are identified by (UPS) by the presence of C-C and C-W bonds. Upon heating to $1100^\circ K$, the C-C bond breaks and carbon atoms remain on the surface in a disordered state.

One of the striking features of the adsorption process is the existence of small (of the order of kT) activation energy barriers in the path of various bond breaking reactions. As a result an organic molecule may be adsorbed intact even on the most reactive metal surface at sufficiently low surface temperatures. As the temperature is increased, electron spectroscopy can be used to identify the different bond breaking processes that seem to occur in readily distinguishable steps.

C. Results of Electron Absorption Spectroscopy Studies

Surface vibrational modes have been detected in high-resolution energy spectra of backscattered low-energy electrons. In such an experiment, the energy loss of the incident electrons is measured by measuring

the energy distribution of the scattered electrons from the surface or from the adsorbates. Propst and Piper observed characteristic energy losses due to adsorption of a number of simple gases on W (100).⁽⁴⁹⁾ Vibrational bands observed for H₂, N₂, CO and H₂O are listed in their paper. The energy resolution in these experiments of 50 meV did not

allow measurement of peak shift with coverage to be made. However, from the evidence on CO adsorption on tungsten (100), these authors concluded that the absence of molecular vibrational bands for strongly bound CO indicated that dissociation of this molecule occurs.

More recently Ibach and co-workers^(50, 51, 52) have developed much more sensitive adsorption techniques where the energy resolution is ± 7 meV. They have confirmed the finding that, in fact, CO adsorbed dissociatively on tungsten surfaces. They have also studied zinc oxide and silicon surfaces and observed surface modes of lattice vibrations from both of these surfaces. In addition, vibrational modes of adsorbed oxygen were observed on silicon (111). Electron adsorption studies were carried out also on platinum surfaces in addition to tungsten surfaces. Hydrogen was detected on metal surfaces by its stretching modes of vibration of its bonds to the metal atoms. This technique appears to be one of the most promising in studies of the surface chemical bonds of hydrogen since it detects this atom in the adsorbate states very well indeed. Other techniques of electron scattering have failed to detect hydrogen directly due to the low scattering cross section of this atom as compared to the other atoms in the periodic table.

Studies of CO Bonding

The chemisorption of CO was studied on several metal surfaces by electron spectroscopy. Using synchrotron radiation, Shirley, et al have found that CO adsorbed in a bridge structure bound through the carbon to the metal on the platinum (111) crystal face, while the oxygen end of the molecule is pointing away from the surface.⁽⁵³⁾ Using the high Miller index (775) surface that has a large concentration of kink atoms of low coordination

-21-

number, Mason et al found that the CO dissociates at the kink sites,⁽⁵⁴⁾ while the carbon monoxide does not dissociate on atoms in terrace sites. These studies were carried out using (UPS) and (XPS) techniques. The concentration of carbidic carbon was equal to the kink concentration and was produced at the initial stages of CO chemisorption on this kinked, high Miller index platinum surface. Thus, the adsorption of CO takes place first at kink sites where the molecule dissociates. Once the kinks are blocked by carbon, CO further chemisorbed in the molecular state on the other atomic sites of the heterogeneous platinum surface. CO adsorbed in several bonding sites, some of them molecular, some of them dissociated on tungsten crystal surfaces.⁽⁵⁵⁾

Conclusion

There are several important findings that have come out of LEED and electron spectroscopy studies of the chemical bonding of adsorbates on solid surfaces. Surface crystallography has revealed that many small atoms (O, S, Se, Na) occupy high symmetry surface sites at atomic distances characteristic of a covalent bond to the nearest neighbor metal atoms. Acetylene forms π -d bonds and located at high symmetry sites and at atomic distances that are similar to that found in metallo-organic cluster compounds. Surface irregularities, steps and kinks at surfaces have distinctly different bonding characteristics and chemical reactivities for many solids as compared to atoms on surface terraces. Both the bonding characteristics of adsorbates and the marked changes of chemical activity with coordination numbers of surface atoms, point to the predominance of localized bonding of adsorbates. The surface bond may be viewed as between the adsorbed species and its nearest neighbor surface atoms and to the first approximation interactions with more distant metal atoms can be neglected. The

adsorbed atom or molecule can be looked at as part of a surface molecule or surface cluster that forms between the adsorbed species and its nearest neighbor surface atoms. As a result, strong correlations between the chemistry of polynuclear clusters and that of adsorbed surface species is expected. Future studies will certainly verify the validity of this physical picture of the surface chemical bond.

REFERENCES

1. G. A. Somorjai, S. Hagstrom and H. B. Lyon, Phys. Rev. Lett. 15, 491 (1965).
2. G. A. Somorjai and A. E. Morgan, Surf. Sci. 12, 405 (1968) and G. A. Somorjai and A. E. Morgan, J. Chem. Phys. 51, 3309 (1969).
3. T. A. Clark, R. Mason and M. Tescari, Surf. Sci. 30, 553 (1972).
4. D. G. Fedak and N. A. Gjostein, Surf. Sci. 8, 77 (1967).
5. J. T. Grant, Surf. Sci. 18, 223 (1969).
6. H. P. Bonzel and R. Ku, J. Vac. Sci. Technol. 9, 663 (1972).
7. L. L. Kesmodel and G. A. Somorjai, Accts. Chem. Res. (To be published).
8. G. A. Somorjai and H. R. Martin, Phys. Rev. B 7, 3607 (1973).
9. J. A. Strozier, Jr., D. W. Jepsen and F. Jona, In Surface Physics of Materials, Vol. I, edited by J. M. Blakely (Academic, New York, 1975).
10. M. A. Van Hove and S. Y. Tong, Surf. Sci. 54, 91 (1976).
11. J. R. Arthur, Surf. Sci. 43, 449 (1974).
12. H. H. Brongersma and P. M. Mul, Surf. Sci. 35, 393 (1973).
13. See, for example, the series of three papers by T. E. Gallon, I. G. Higginbotham, M. Prutton and H. Tokutaka, Surf. Sci. 21, 224 (1970), and references therein.
14. G. A. Somorjai and T. M. French, J. Phys. Chem. 74, 2439 (1970).
15. L. Fiermans and J. Vennik, Surf. Sci. 18, 317 (1969).
16. L. E. Firment and G. A. Somorjai, Surf. Sci. 55, 413 (1976).
17. L. E. Firment and G. A. Somorjai, J. Chem. Phys. (To be published).
18. J. Buchholz and G. A. Somorjai, J. Chem. Phys. (To be published).
19. D. W. Blakely and G. A. Somorjai, Nature 258, 530 (1975).

20. G. A. Somorjai, S. L. Bernasek and W. J. Siekhaus, *Phys. Rev. Lett.* 30, 1202 (1973).
21. H. Ibach, K. Horn, R. Dorn and H. Lüth, *Surf. Sci.* 38, 433 (1973).
22. G. A. Somorjai and D. W. Blakely, *J. Catalysis* 42, 181 (1976).
23. J. Perdureau and G. E. Rhead, *Surf. Sci.* 24, 555 (1971).
24. M. Henzler, *Surf. Sci.* 19, 159 (1970).
25. W. P. Ellis and R. L. Schwoebel, *Surf. Sci.* 11, 82 (1968).
26. B. Krahl-Urban and H. Wagner, *Phys. Electronics Conf.*, June 7-9, 1976, Madison, Wisconsin.
27. L. L. Kesmodel and L. M. Falicov, *Solid State Comm.* 16, 1201 (1975).
28. Y. W. Tsang and L. M. Falicov, *J. Phys. C.* 9, 51 (1976).
29. G. A. Somorjai and L. L. Kesmodel, in International Review of Science, Physical Chemistry Series Two, Vol. 7, Surface Chemistry and Colloids, edited by H. Kerker (Butterworths, London, 1975).
30. J. B. Pendry, *J. Phys. Chem.* 2, 2273 (1973); 2, 2283 (1969).
31. P. C. Stair, T. J. Kaminska, L. L. Kesmodel and G. A. Somorjai, *Phys. Rev. B* 11, 623 (1975).
32. K. Siegbahn, et al., ESCA-Atomic, Molecular and Solid State Structure Studied by Means of Electron Spectroscopy (Almqvist and Wiksells, Uppsala, 1967).
33. E. G. McRae and H. D. Hagstrum in Treatise on Solid State Chemistry, Vol. 6A, edited by H.B. Hannay (Plenum Press, New York, 1976).
34. See, for example, C. C. Chang, *Surf. Sci.* 25, 53 (1971). or
G. A. Somorjai and F. J. Szalkowski, *Adv. High Temp. Chem.* 4, 137 (1971).
35. R. L. Park and J. E. Houston, *J. Vac. Sci. Technol.* 11, 1-13 (1974).
36. See, for example, D. E. Eastman, in Electron Spectroscopy, edited by D. A. Shirley (North Holland, New York, 1972).

37. H. Ibach, J. Vac. Sci. Technol. 9, 713 (1972).
38. S. Andersson and J. B. Pendry, J. Phys. C 5, L41 (1972).
39. J. E. Demuth, D. W. Jepsen and P. M. Marcus, Phys. Rev. Lett. 31, 540 (1973).
40. F. Forstmann, W. Berndt and P. Buttner, Phys. Rev. Lett. 30, 17 (1973).
41. M. Van Hove and S. Y. Tong, presented at the 1975 Physical Electronics Conference, State College, Pennsylvania, Phys. Rev. Lett. 35, 1092 (1975).
42. A. Ignatiev, F. Jona, D. W. Jepsen and P. M. Marcus, Surf. Sci. 49, 189 (1975).
43. J. E. Demuth, Progress in Colloid and Surface Science (To be published 1977).
44. H. D. Shih, F. Jona, D. W. Jepsen and P. M. Marcus, Phys. Rev. Lett. 36, 14 (1976).
45. P. C. Stair and G. A. Somorjai, Chem. Phys. Lett. 41, 391 (1976).
46. L. L. Kesmodel, P. C. Stair, R. C. Baetzold and G. A. Somorjai, Phys. Rev. Lett. 36, 1316 (1976).
47. J. E. Demuth and D. E. Eastman, Phys. Rev. B, 1523 (1976).
48. E. W. Plummer, B. J. Wacławski and T. V. Vorburger, Chem. Phys. Lett. 23, 510 (1974).
49. F. M. Propst and T. C. Piper, J. Vac. Sci. Technol. 4, 53 (1967).
50. H. Frotzheim, H. Ibach and S. Lehwald, "Surface Sites of H on W (100)", (To be published).
51. H. Frotzheim, H. Ibach and S. Lehwald, "Surface Vibrations of CO on W (100)", (To be published).
52. H. Frotzheim, H. Ibach and S. Lehwald, "Surface Vibrations of Oxygen on W (100)", (To be published).

53. D. A. Shirley, et al, Phys. Rev. Lett. (To be published).
54. R. Mason and G. A. Somorjai, J. Amer. Chem. Soc., (To be published).
55. T. Yates, N. E. Erickson, S. D. Worley and T. E. Hadey in The Physical Basis for Heterogeneous Catalysis, p. 75 (Plenum Press, New York, 1975).

FIGURE CAPTIONS

- Figure 1 - (a) Diffraction pattern from the Pt (100) - (5x1) structure;
(b) Schematic representation of the (100) surface with a hexagonal overlayer;
(c) Diffraction pattern from the Pt (100) - (1x1) structure;
(d) Schematic representation of the (100) surface.
- Figure 2 - Model of a solid surface on an atomic scale.
- Figure 3 - A low-energy electron diffraction apparatus of the post-acceleration type. Grids A and C are at ground potential for shielding purposes, and a voltage nearly equal to the gun accelerating potential is placed on grid B so that only the elastically backscattered electrons may pass through it. These electrons are then post-accelerated to a phosphor screen for observation through the viewport.
- Figure 4 - Schematic indicating various high-symmetry local bonding sites for acetylene on the (111) face of an f.c.c. crystal: (a) one-coordinate π , (b) di- σ , (c) bridging, (d) triangular.
- Figure 5 - Comparison of calculated I-V profiles for various model geometries ($z=1.9 \overset{0}{\text{Å}}$) to experiment (stable acetylene overlayer) for two fractional-order beams.
- Figure 6 - Comparison of calculated I-V profiles for various model geometries ($z=1.9 \overset{0}{\text{Å}}$) to experiment (stable acetylene overlayer) for two integral-order beams.

Table I
Adsorbate-Substrate Bond Lengths Determined by LEED

Substrate	Adsorbate	Bond Length (experimental)	Ref.	Bond Length (predicted) ¹⁸
Ni(001)	O	1.97Å	a	1.90Å
	S	2.18Å	a	2.28Å
	Se	2.27Å	a	2.41Å
	Te	2.58Å	a	2.61Å
	Na	3.37Å	b	3.10Å
Ni(110)	O	1.91Å	c	1.90Å
	S	2.17Å	d	2.28Å
Ni(111)	S	2.02Å	d	2.28Å
Ag(001)	Se	2.80Å	e	2.61Å
Ag(111)	I	2.75Å	f	2.77Å
Al(100)	Na	3.52Å	g	3.32Å
Mo(001)	N	2.02Å	h	2.08Å
W(110)	O	2.08Å	i	2.05Å

^a F. Forstmann, W. Berndt and P. Buttner, Phys. Rev. Lett., 30, 17 (1973).

^b J. E. Demuth, D. W. Jepsen and P. M. Marcus, Phys. Rev. Lett., 32, 1132 (1974).

^c B. H. Hutchins, T. H. Rhodin and J. E. Demuth, Presented at the 1975 American Physical Society Meeting, Denver, Colorado.

^d H. Van Hove and S. Y. Tong, Phys. Rev. Lett. 35, 1092 (1975).

^e L. L. Kesmodel, P.C. Stair and G. A. Somorjai, To be published.

- ^f A. Ignatiev, F. Jona, D. W. Jepsen and P. H. Marcus, *Surface Sci.* 49, 189 (1975).
- ^g J. L. Gland and G. A. Somorjai, *Surface Sci.* 38, 157 (1973); *Surface Sci.* 41, 387 (1974).
- ^h J. E. Demuth, D. W. Jepsen and P. H. Marcus, Presented at the 1975 Physical Electronics Conference, State College, Pa.
- ⁱ L. Pauling, The Chemical Bond, (Cornell University Press, Ithaca, N. Y., 1967).

Table II. Examples of bonding structures and bond lengths for acetylenic ligands ($RC \equiv CR$) in various transition-metal complexes.

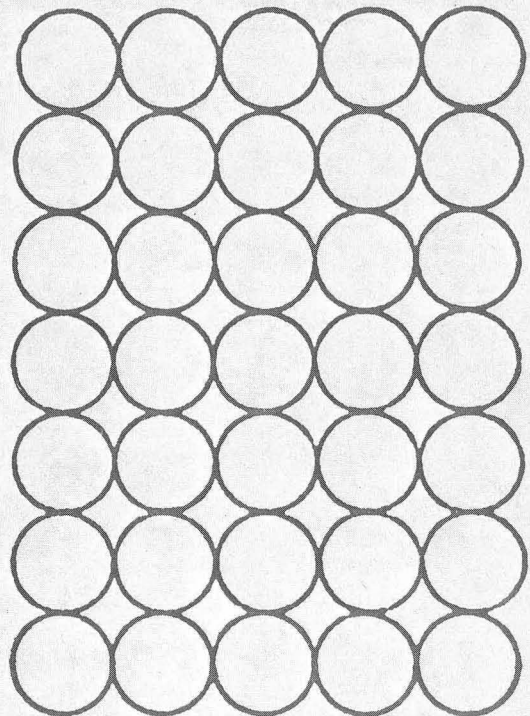
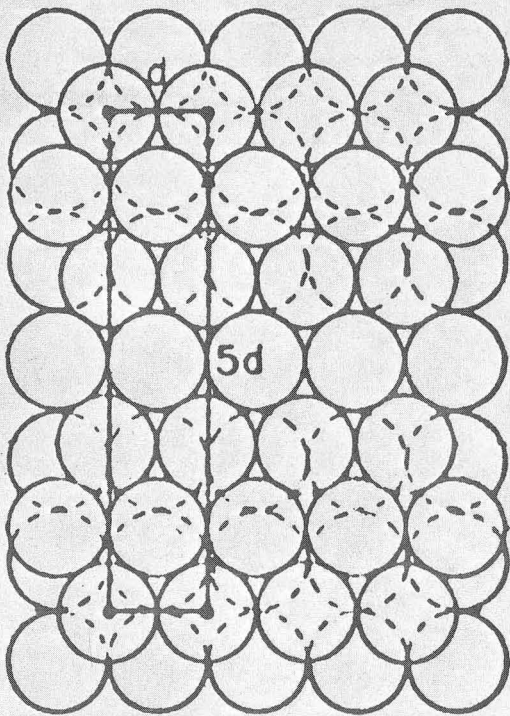
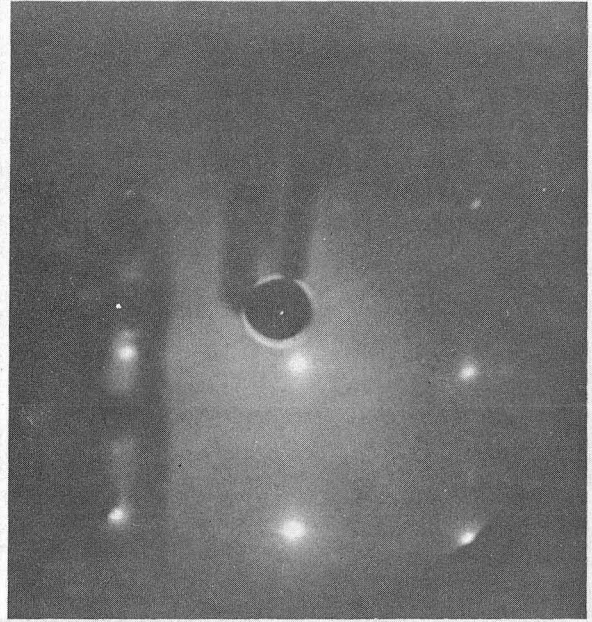
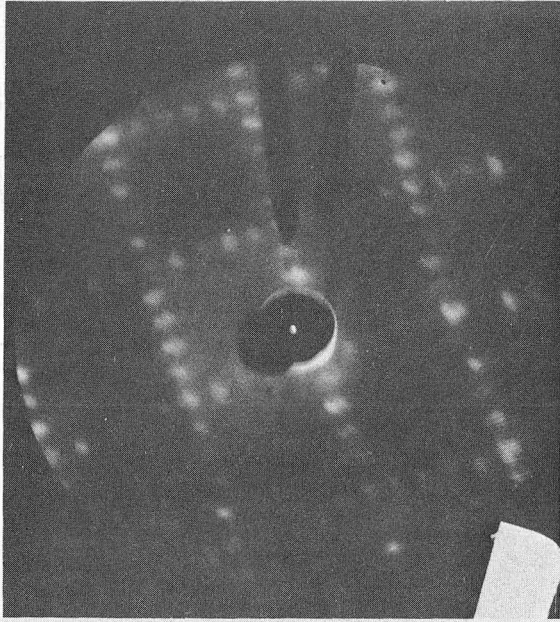
<u>Compound</u>	<u>Bonding Geometry</u>	<u>Average M-C (Å)</u>	<u>C≡C (Å)</u>
$(Ph_3P)_2Pt(C_2Ph_2)^a$	one-coordinate π	2.04	1.32
$(CO)_6Co_2(C_2Ph_2)^b$	bridging (μ)	1.97	1.46
$(h^5-C_5H_5)_2Rh_2(CO)_2(CF_3C_2CF_3)^c$	di- σ	2.04	1.29
$Os_3(CO)_{10}(C_2Ph_2)^d$	triangular	2.22	1.29

^a J. O. Glanville, J. H. Stewart, and S. O. Grim, *J. Organometal. Chem.* 7, P9 (1967).

^b W. G. Sly, *J. Am. Chem. Soc.* 81, 18 (1959).

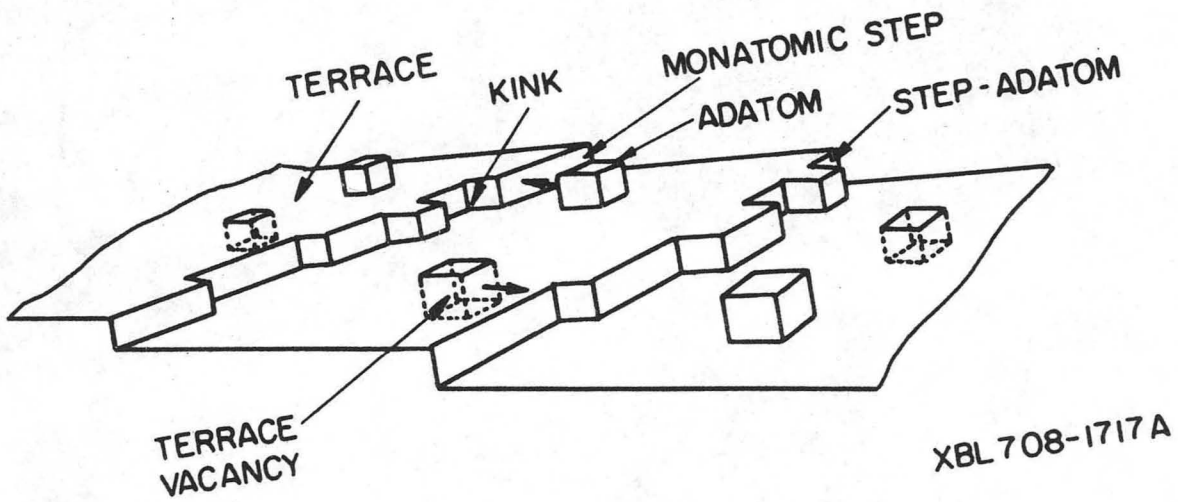
^c R. S. Dickson, H. P. Kirsch, and D. J. Lloyd, *J. Organometal. Chem.* 101, C48 (1975).

^d M. Tachikawa, J. R. Shapley, C. G. Pierpont, *J. Am. Chem. Soc.* 97, 7174 (1975).



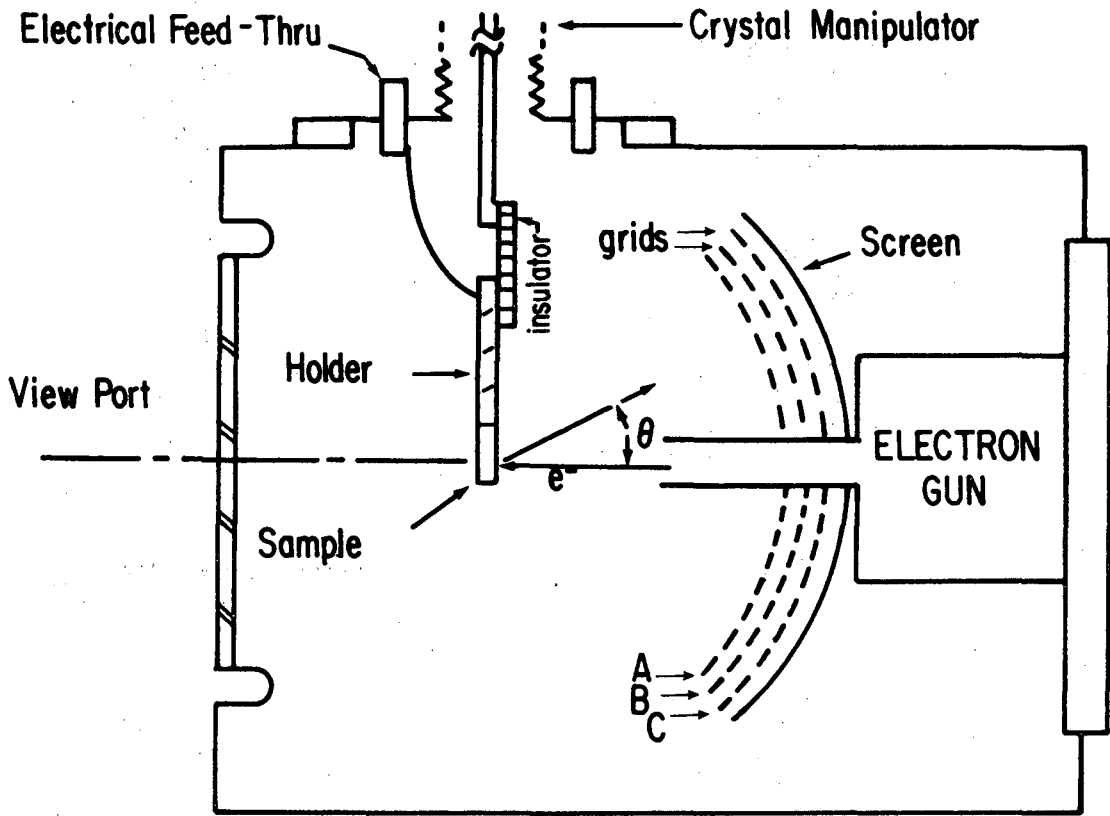
XBB 711-5356

Fig. 1



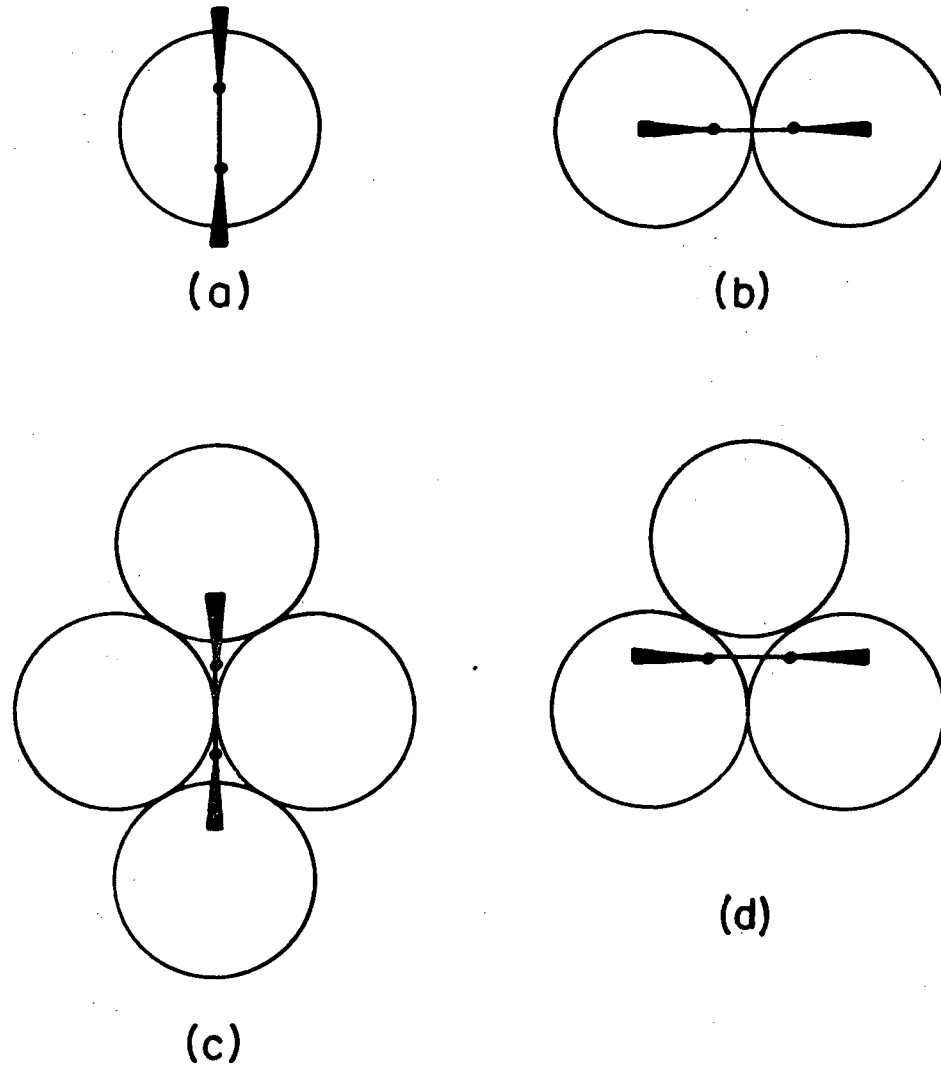
XBL 708-1717 A

Fig. 2



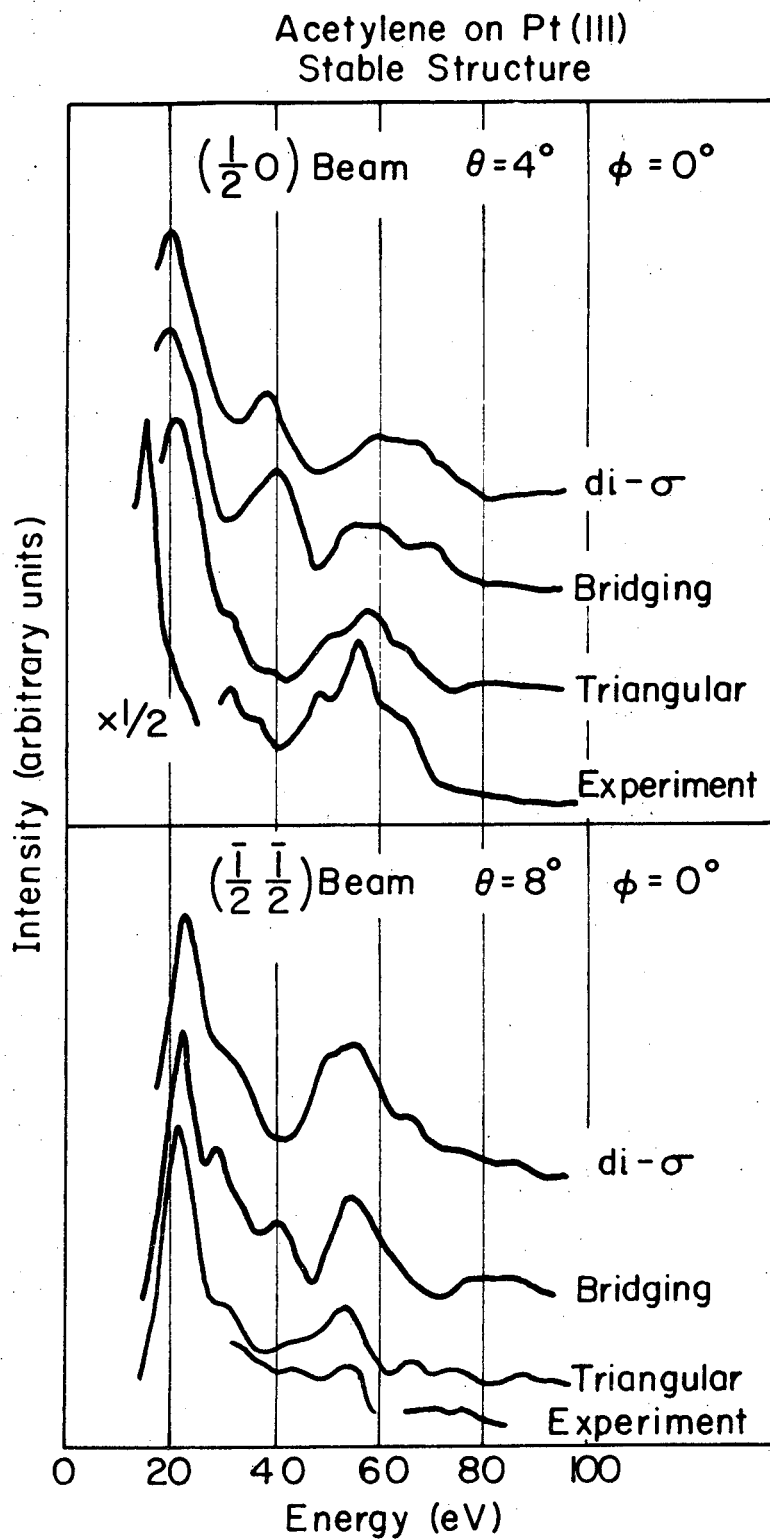
XBL 703-556

Fig. 3



XBL 767-7141

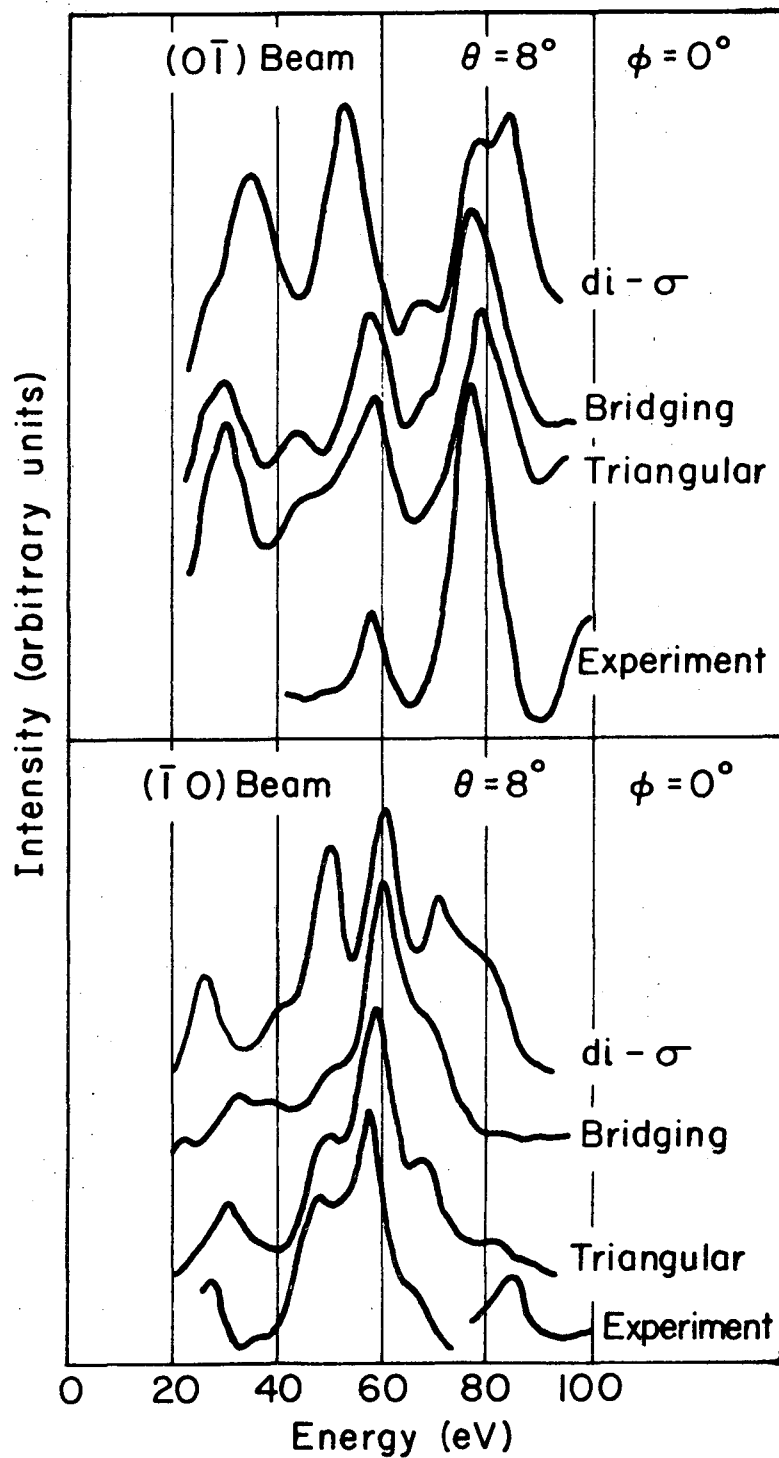
Fig. 4



XBL 767-7145

Fig. 5

Acetylene on Pt(111)
Stable Structure



XBL 767-7146

Fig. 6

This report was done with support from the United States Energy Research and Development Administration. Any conclusions or opinions expressed in this report represent solely those of the author(s) and not necessarily those of The Regents of the University of California, the Lawrence Berkeley Laboratory or the United States Energy Research and Development Administration.

TECHNICAL INFORMATION DIVISION
LAWRENCE BERKELEY LABORATORY
UNIVERSITY OF CALIFORNIA
BERKELEY, CALIFORNIA 94720